Ultrasonics Sonochemistry 19 (2012) 1120–1125

Contents lists available at SciVerse ScienceDirect

Ultrasonics Sonochemistry

journal homepage: www.elsevier.com/locate/ultsonch

Phase transitions of nanoemulsions using ultrasound: Experimental observations

Ram Singh [a], Ghaleb A. Husseini [b], William G. Pitt [a,*]

[a] Chemical Engineering Department, Brigham Young University, Provo, UT 84602, USA
[b] Chemical Engineering Department, American University of Sharjah, Sharjah, United Arab Emirates

ARTICLE INFO

Article history:
Received 2 October 2010
Received in revised form 29 October 2011
Accepted 13 February 2012
Available online 1 March 2012

Keywords:
Perfluorocarbons
Ultrasound
Cavitation
Nanoemulsions
Microbubbles

ABSTRACT

The ultrasound-induced transformation of perfluorocarbon liquids to gases is of interest in the area of drug and gene delivery. In this study, three independent parameters (temperature, size, and perfluorocarbon species) were selected to investigate the effects of 476-kHz and 20-kHz ultrasound on nanoemulsion phase transition. Two levels of each factor (low and high) were considered at each frequency. The acoustic intensities at gas bubble formation and at the onset of inertial cavitation were recorded and subsequently correlated with the acoustic parameters.

Experimental data showed that low frequencies are more effective in forming and collapsing a bubble. Additionally, as the size of the emulsion droplet increased, the intensity required for bubble formation decreased. As expected, perfluorohexane emulsions require greater intensity to form cavitating bubbles than perfluoropentane emulsions.

1. Introduction

Ultrasound (US), defined as a sound wave at a frequency of at least 20 kHz, is an effective modality for drug delivery because it can be noninvasively focused on the desired tissue volume. Most drug delivery techniques do not employ such specific targeting in time and space as is available with ultrasound. The unique advantages of ultrasonic drug delivery make it convenient for localized delivery to tumors and to specialized organs such as the heart, eyes, and brain [1–4].

Acoustic cavitation is the formation and subsequent oscillation of bubbles in an acoustic field. Ultrasonic cavitation perturbs cell membrane structure and thus increases its permeability to drugs and other solutes by several mechanisms including enhanced transport to the cell and increased transmembrane transport. For example, cavitation transiently disrupts the cell membrane and forms pores therein [5–8]. Ultrasound has been used for drug and gene delivery *in vivo* and *in vitro* [6,9–11].

There are two general types of acoustic cavitation that pertain to drug and gene delivery: stable and inertial cavitation. Stable cavitation refers to the continuous and relatively low amplitude oscillation of bubbles in response to oscillating pressure, whereas inertial (or collapse) cavitation refers to the nearly total volumetric collapse of bubbles exposed to US at high pressure amplitudes or when the bubble is near its resonant size [12,13]. Both mechanisms enhance transport and can facilitate drug and gene delivery. For example, stable oscillating bubbles create very strong fluid shear stress near the surface of the bubble, sufficient to shear cell membranes. Inertial cavitation additionally creates shock waves and fluid microjets, which also disrupt cell membranes. Another important distinction between stable and inertial cavitation is that at low frequencies, less acoustic amplitude is required to produce inertial cavitation [14]. The propensity for inertial cavitation to occur is indicated by the mechanical index (MI), which takes into account the relationship between frequency and cavitation mode [15]. The MI is defined as the ratio of the peak negative pressure in MPa to the root of the frequency in MHz: $MI = (P^{-}/\mathrm{MPa})/\sqrt{f/\mathrm{MHz}}$. Values of MI above 0.3 are likely to be associated with inertial cavitation [16].

Ultrasonic drug and gene delivery are enhanced by the presence of pre-formed bubbles [17–20]. Such bubbles can be produced by mixing gas into liquid or by vaporizing liquid into gas. Our specific interests lie in the vaporization of liquid perfluorocarbon (PFC) droplets which produces rapidly expanding and perhaps oscillating gas bubbles [21–23]. There are several recent reports regarding the use of ultrasound to transform superheated perfluorocarbon (PFC) liquid droplets into gas bubbles for various biomedical purposes including drug delivery and blood vessel occlusion [24–26].

Stabilized PFC liquid droplets have been produced and examined *in vivo* for diagnostic or therapeutic purposes [18,27–30]. For example, micro-sized perfluoropentane droplets stabilized by an albumin coating did not vaporize even when slightly above their boiling point, but remained as superheated droplets with useful ultrasound contrast properties. However, under some conditions these super-heated droplets can be vaporized by US into larger gas bubbles [31–33].

* Corresponding author. Tel.: +1 801 422 2589; fax: +1 801 422 0151.
E-mail address: pitt@byu.edu (W.G. Pitt).

1350-4177/$ - see front matter © 2012 Elsevier B.V. All rights reserved.
doi:10.1016/j.ultsonch.2012.02.005

Since a PFC gas has low solubility in water, it is often used in US contrast agents because it dissolves much more slowly than air bubbles. Commercial contrast agents such as Optison, Definity, and EchoGen that employ these PFC gases have significantly increased lifetimes [34,35].

A limitation of these PFC gas bubbles is that their size (~5 μm diameter) precludes them from penetrating through the capillaries walls in tumors to the tissue beyond, and thus any type of US-induced drug or gene therapy is limited to the surface and internal volume of the circulatory system. However, it is desirable to extend drug and gene delivery to tissues beyond the capillaries. Capillaries consist of only a single layer of endothelial cells. In most tissues these cells are tightly connected to each other, effectively preventing penetration of gas bubbles into the tissue. However, many tumors have a porous and unorganized capillary vasculature that allows vesicles of less than 300 nm in diameter to penetrate their capillaries [36].

Although PFC gas bubbles are too large to extravasate, liquid PFC emulsion particles of sufficiently small size are able to penetrate beyond the capillaries in some tumor tissues. An overall goal of our research is to exploit the physics and chemistry in a novel method, whereby ultrasound is used to produce cavitation bubbles from liquid PFC emulsions of a size that can penetrate beyond the leaky capillaries in a tumor. More specifically the purpose of this study is to understand the physics and chemistry of phase transition of sub-micron-sized perfluoropentane (PFC_5) and perfluorohexane (PFC_6) nanoemulsions subjected to 20-kHz and 476-kHz ultrasound frequencies.

Fig. 1 illustrates the local pressure variation as ultrasound propagates in a medium, generating positive and negative pressure (relative to the local hydrostatic pressure) in a cyclic way and oscillates around atmospheric pressure. When rarefaction pressure of the wave drops below the vapor pressure of PFC_6 (29.1 kPa at 25 °C) for a sufficient time, perfluorohexane evaporates and forms a gas phase. Sufficient time means that the local pressure is lower than the vapor pressure for a sufficient time to produce heterogeneous or homogeneous nucleation of the gas phase. Water vapor pressure is 3.17 kPa at 25 °C, much lower than the PFC_6 vapor pressure. Therefore, it is hypothesized that the first bubbles to form are mostly PFC with about 10% water vapor.

Similarly PFC_5, with a vapor pressure of 87.6 kPa at 25 °C, may commence phase transition much earlier and for a longer time during the acoustic cycle. In this case, the first gas to form would contain about 97% PFC_5.

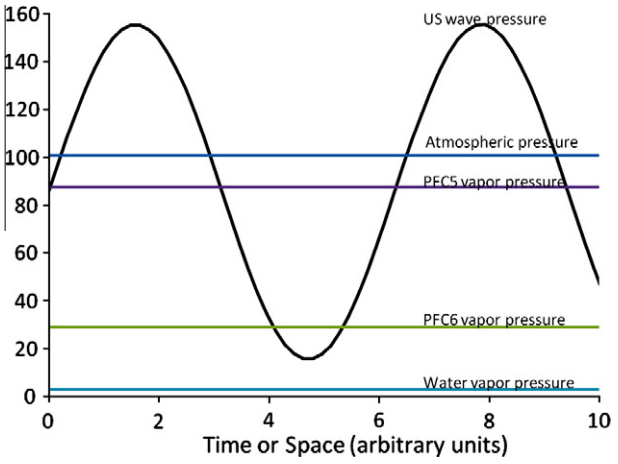

Fig. 1. The local pressure (kPa) in a medium oscillates as ultrasound wave propagates through the medium. The horizontal lines represent the vapor pressures of PFC_6, PFC_5, and water at 25 °C. When the local pressure falls below the vapor pressure of a liquid present, vaporization can occur. Water has the lowest vapor pressure among components of the perfluorocarbon emulsions.

A further complication is that the pressure inside a nanoemulsion droplet is always greater than the surrounding liquid pressure because of the additional contribution from the Laplace pressure: $\Delta P = \frac{2\gamma}{r}$, where γ is interfacial energy. The Laplace pressure can become very large as the nanoemulsions become very small. As the local pressure drops below the vapor pressure of the PFC less the Laplace pressure, the PFC becomes superheated (or sub-pressurized) and there is a driving potential to nucleate a gas phase. However, if the acoustic cycle is sufficiently short or the sub-pressurization is inadequate, no gas phase will form. Unfortunately, the kinetics of PFC gas nucleation from liquid droplets are not found in literature, so one cannot predict the length of time or magnitude of sub-pressurization required to nucleate the gas phase.

Our research group has experimentally monitored the formation and behavior of gas bubbles by listening to the acoustic emissions of the system. The acoustic emissions of bubbles are Fourier transformed to produce a frequency spectrum of the emission. If no bubbles are present, only the applied (fundamental) signal is heard. The formation and stable oscillation of gas bubbles are indicated by the appearance of higher harmonics in the acoustic emissions. Moreover, the appearance of ultraharmonics and subharmonics indicate vigorous bubble oscillations near or at the onset of inertial cavitation [37,38], while inertial cavitation itself is indicated by a broadband background white noise [16,39]. These acoustic signatures were used to study the acoustic amplitudes that created gas formation in PFC emulsions, and the subsequent behavior of the nucleated bubbles. In particular, we studied these transitions as a function of PFC emulsion temperature, size and chemistry.

2. Materials and methods

2.1. Preparation of nanoemulsions

Nanoemulsions of 250-nm diameter and 550-nm diameter of perfluorohexane (Fluka 77273, Sigma–Aldrich, St. Louis, MO) and perfluoropentane (PC6182, Apollo Scientific Ltd.) were prepared in degassed distilled deionized water (ddd-H_2O). The ddd-H_2O was prepared in a vacuum chamber at 3.1 kPa for 5 min. Perfluorooctanoic acid (PFOA, 171468-25G, Sigma–Aldrich, Saint Louis, MO) was used as a stabilizing surfactant. To produce 250-nm or 550-nm emulsions, different ratios of surfactant to perfluorocarbon were prepared in ddd-H_2O. Emulsions were prepared in a 2-mL glass vial (952674, XPERTEK, St. Louis, MO) as follows. A cylindrical glass basin about 5.1 cm deep by 22.9 cm wide was filled with ddd-H_2O. Aluminum caps with rubber septa were submerged in the ddd-H_2O. With a clean 20-gauge needle and 5-mL syringe, water was squirted into the submerged caps to remove any attached air bubbles. A dry 2-mL vial was weighed and the desired masses of PFOA powder and PFC liquid were placed into the vial, along with a 14-mm Teflon-coated metal bar. One milliliter of ddd-H_2O was added drop by drop from a syringe to wash down PFOA on the sides of the vial. Then the remainder of the vial was carefully filled with ddd-H_2O. The vial was submerged upright in the ddd-H_2O in the basin. One of the caps already submerged in the water was picked up carefully and placed over the vial without allowing the cap to come out of the water (thus preventing any air from entering the cap). The cap was crimped in place underwater with a hand crimper.

After crimping, the vial was removed from the water bath and carefully examined to ensure absence of any air bubbles. If any gas bubbles were visible, the lid was removed, the bubble was removed, and the whole capping procedure was repeated or the entire sample was discarded. To produce the emulsion, the vial

was subjected to mechanical mixing in a cap mixer (TP-103 Amalgamator, GC America, Inc., Alsip, IL) for 20 s. The Teflon bar in the vial created high shear during the mixing, which emulsified the vial contents.

Removal of the nanoemulsion from the vial was done by positive displacement instead of by suction with a syringe. A 25-gauge needle was inserted so the tip was in the middle of the vial. Then a syringe containing air was capped with another 25-gauge needle and inserted through the septum into the vial. The air was slowly pushed into the vial which pushed the emulsion into the hub of the first needle. This emulsion was extracted from the hub with a 200-μL pipette and transferred into ddd-H_2O for dilution. Thus the emulsion remained free of gas bubbles.

The size and stability of the emulsions were characterized by a dynamic light scattering (DLS) instrument (BI-9000AT/90Plus, Brookhaven Instruments Corporation, Austin, TX). Three samples of each emulsion were emulsified at the same time and measured one by one in the DLS instrument at 10 min intervals to determine emulsion stability.

2.2. 476-kHz Experimental setup

The chamber used to expose the nanoemulsions to 476-kHz ultrasound was an aluminum box of ~2 L volume lined with acoustically absorbing rubber on the bottom and sides. Placed on one wall was a 476-kHz ultrasonic transducer (Sonic Concepts, Woodinville, WA). A continuous sine wave at 476 kHz–produced by a signal generator (Hewlett Packard, model 33120A) was sent to a power amplifier (ENI Model 240L, Rochester, NY), which in turn sent the amplified signal through a matching network to the ultrasonic transducer. Using the above setup, our nanoemulsions were exposed to 476-kHz ultrasound to determine the intensities required to form cavitating gas bubbles. Each emulsion was diluted to 5% by volume with ddd-H_2O and placed in a thin-walled polyethylene bulb (12-mm diameter transfer pipette), which is nearly transparent to ultrasound. The polyethylene bulb was placed at the focal point of the transducer, and ultrasound at 476 kHz and various intensities were applied to these emulsions. Sufficient water was added to the water bath before each experiment so that the bulb always stayed immersed 30–40 mm below the water surface. An ONDA (model HNR-1000) hydrophone was placed adjacent to the sample and used to capture the acoustic emissions and measure the power density. The nanoemulsions were insonated for 10–20 s.

An oscilloscope (Tektronix, Beaverton, OR) was used to monitor, capture, and Fourier transform the acoustic emissions. Special care was taken to prevent impurities or dissolved gases from nucleating cavitation bubbles in the water surrounding the sample; this was done by recirculating the water from a thermostatic bath and through a 0.2-μm filter. The temperature of the water was controlled at 25 °C or 37 °C.

In a typical experiment at 476 kHz, the US intensity was turned to its lowest value, and the Fourier transforms of the emissions were displayed on the oscilloscope. Then the intensity was slowly increased. The phase transition from liquid to gas and to the various gas bubbles cavitation modes were monitored by observing the Fourier transformed signal of the acoustic emissions. Initially, the Fourier transform data displayed only one peak at the applied frequency of 476 kHz. The absence of other peaks indicated the absence of gas bubbles oscillating nonlinearly and producing higher harmonic peaks. While slowly increasing the amplitude of the ultrasound, the second harmonic ($2f$), and third harmonic ($3f$), and higher harmonics (nf, $n = 2, 3, 4\ldots$) started appearing on the oscilloscope. Even further increase of amplitude produced ultraharmonic $f(n + 1/2)$ and subharmonic (f/n) peaks, usually at $f/2$ and sometimes at $f/3$ or $2f/3$. Finally, there was a slight baseline shift which signaled the onset of inertial cavitation producing white noise. The acoustic intensity was recorded at the first sign of harmonics, ultraharmonics, subharmonics, and baseline shift. The ultraharmonics and subharmonic signals nearly always appeared simultaneously.

2.3. 20-kHz Experimental set-up

For 20-kHz experiments, we used a glass tank of 75 L capacity. The tank was lined with ultrasound-absorbing rho-C rubber on the inside. Water in the tank was heated by two fish tank heaters and maintained at a constant temperature of 25 °C or 37 °C. The emulsion sample was diluted to 5% by volume with ddd-H_2O in a polyethylene bulb. Then the polyethylene bulb was inserted into a floating stage that kept the sample in a vertical up-right position such that the center of the bulb was 10 mm below the water surface. The 20-kHz transducer (3 mm stepped microtip, Sonics and Materials, Newtown, CT) was positioned so that the tip of transducer remained immersed 10 mm under the surface of the water. During the experiments the tip of the transducer was placed in the center of the bulb containing the sample. Mounted 25 mm horizontally from the center of the sample bulb in the 20-kHz experiments was a low frequency hydrophone (Model 8103, Bruel & Kjaer, Nærum, Denmark), which collected the acoustic emissions. The hydrophone was connected to an oscilloscope that Fourier-transformed and stored the acoustic signals acquired by the hydrophone.

Similarly to the previously described experiments, the Fourier transform of the 20-kHz spectrum was displayed on the oscilloscope. Even at the lowest amplitude setting of the 20-kHz instrument, we observed the fundamental with a small component of higher harmonics. On further increase in amplitude, the ultraharmonic and subharmonic signals appeared, which was accompanied with a strong upward baseline shift. Again the acoustic amplitudes producing the transitions were recorded.

To calculate the power density of ultrasound at the transitions of bubble behavior the RMS voltage (V_{rms}) of the hydrophone was recorded from the oscilloscope and was converted into intensity (W/cm^2) values.

3. Results

Experiments were conducted at 476 kHz and 20 kHz for two different temperatures, two different sizes of emulsion droplets (250 and 550 nm), and two different perfluorocarbons (PFC_5 and PFC_6). The emulsion sizes were measured at various mass ratios of surfactant to perfluorocarbon. As expected the size of the emulsions showed a decreasing trend with increasing surfactant ratio. Fig. 2 shows the size data for the PFC_5 emulsions versus the ratio of PFOA to PFC_5.

Although these emulsions were stable for 30–60 min, after 2–3 h, the emulsions start to coalesce. Thus, the average size of emulsion increased if the emulsion was stored for long periods of time. Therefore emulsions were prepared and used within 60 min.

In order to find other surfactants which could give a stable size emulsion of 250 and 550 nm, we experimented with other surfactants such as perfluorooctylbromide, ZONYL-FSO, caprylic acid, butyric acid, Span20, and Pluronic F68. None of these produced a sufficiently stable emulsion to use in this research. We hypothesized that this could be due to the hydrocarbon nature of all but the first of these, which makes them less compatible with the PFC emulsions. The subsequent data were obtained for PFC emulsions stabilized with PFOA.

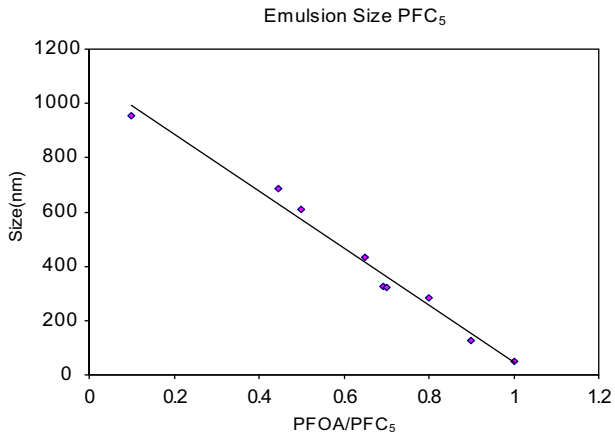

Fig. 2. Perfluoropentane emulsion size decreases with increasing surfactant to PFC_5 ratio.

3.1. Monitoring emulsion and bubble transitions

The acoustic intensity data were correlated with the various transitions in acoustic phenomena. The transition intensities were examined to show the effect of the parameters of temperature, emulsion size and emulsion chemistry. Recall that the appearance of higher harmonics indicates bubble formation and stable cavitation. The baseline shift occurs due to shock waves generated by inertial cavitation of the bubbles.

3.2. Effect of temperature at 476 kHz

In general, the intensity required to produce higher harmonics was about 10-fold greater than the initial observation of the fundamental frequency. The intensity required to produce the baseline shift was about sixfold higher than that required for the higher harmonic frequencies.

The intensity required to observe the fundamental frequency was the same at both temperatures because this signal was present at the lowest intensity possible. Comparison of the exposure of 250-nm perfluorohexane emulsions to 476-kHz US at 25 °C and 37 °C (Fig. 3) showed that the transition to higher harmonics was not very sensitive to temperature and is not statistically significant ($p = 0.093$). However, the intensity required for a baseline shift was slightly less at 37 °C. However, the difference is still not statistically significant ($p = 0.157$).

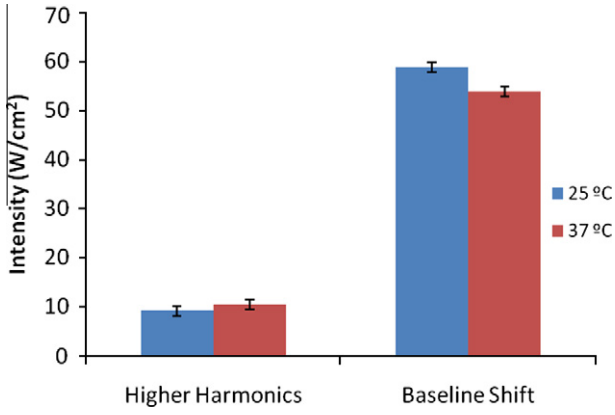

Fig. 3. Effect of temperature on intensity required to see a higher harmonic, and baseline shift. Two hundred and fifty nanometer PFC_6 emulsions were exposed to 476 kHz US at two different temperatures, 25 °C and 37 °C.

3.3. Effect of temperature at 20 kHz

When 250-nm emulsions were exposed to 20-kHz frequency at 25 °C and 37 °C, we observed the same pattern in intensity required to produce the higher harmonic and baseline shift as that seen at 476 kHz. More scatter was observed in this data set compared to that of the 476 kHz (Fig. 4). Again at 20 kHz, the fundamental frequency was always apparent, even at the lowest setting of the transducer, thus the onset of a fundamental frequency is not reported.

The intensity required to produce a baseline shift was only about twice the intensity required for the higher harmonic for the emulsion at 25 °C. For the emulsion at 37 °C, the intensity required to produce a baseline shift was approximately 20% higher than the intensity required producing the higher harmonic frequencies. At 20 kHz, the intensity required to produce transitions is not statistically higher at 25 °C for higher harmonics ($p = 0.058$), but it is statistically higher for a baseline shift ($p = 0.026$).

3.4. Effect of initial emulsion size on onset intensities

On exposure of 250-nm and 550-nm perfluorohexane emulsions to 20-kHz US at 25 °C, the intensity required to produce gas bubbles was greater for the smaller emulsion size. This can be attributed to the Laplace pressure, which is higher for the smaller emulsion size, so more intensity is required to overcome the Laplace pressure (Fig. 5).

The data in Fig. 5 show that 250-nm emulsions required slightly higher intensity than 550-nm emulsions to form bubbles, but required nearly double the intensity to produce the inertial cavitation evidenced by the baseline shift. The differences in onset intensity are not statistically significant for the onset of higher harmonics ($p = 0.113$), but for the baseline shift, the difference is statistically significant ($p = 0.043$). The 476-kHz experiments at 25 °C showed a similar intensity pattern for the onset of these bubble behaviors, in that higher intensity is required for smaller emulsions ($p = 0.04$, data not shown).

Fig. 6 confirms a lower threshold for the appearance of higher harmonics and a baseline shift for a 250-nm nanoemulsion exposed to 20-kHz ultrasound when compared to the same parameters collected using ddd-H_2O.

3.5. Effect of emulsion size for PFC_5 nanoemulsions at 476 kHz and 37 °C

On exposure of 250-nm and 550-nm PFC_5 nanoemulsions to 476 kHz at 37 °C, there was an increasing trend in intensities

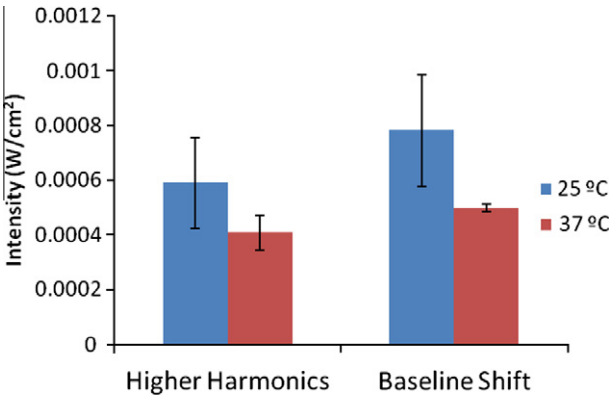

Fig. 4. Temperature effect shown by 20-kHz experiment. Two hundred and fifty nanometer emulsions of PFC_6 were exposed to 20 kHz US at 25 °C and 37 °C.

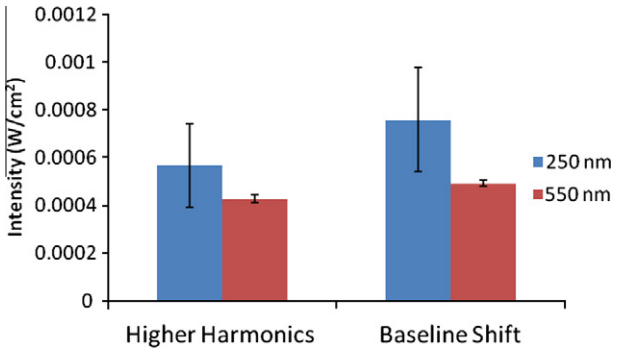

Fig. 5. Effect of emulsion size on bubble behavior in the 20-kHz experiments. 250- and 550-nm PFC_6 emulsions were exposed to 20 kHz US at 25 °C.

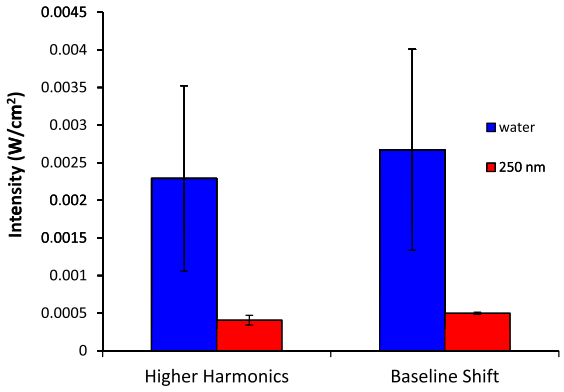

Fig. 6. Transition threshold for ddd-H_2O and 250-nm PFC_6 nanoemulsions at 20-kHz and 37 °C.

(similar to that observed for PFC_6 emulsions) to produce higher harmonics, and a baseline shift (Fig. 7). The intensities for observation of the fundamental are not significantly different for the two nanoemulsions. Statistically significant differences arise, however, at intensities required to view the higher harmonic and the baseline shift. The intensity at the baseline shift for the 250-nm emulsion is almost twice the intensity required at the higher harmonic. The differences in intensity are statistically significant at the onset of higher harmonics ($p = 0.008$) and for a baseline shift ($p = 0.005$). The 20-kHz experiments at 37 °C resulted in similar behavior in that the smaller emulsions required higher intensities to produce the higher harmonics attributed to bubble formation.

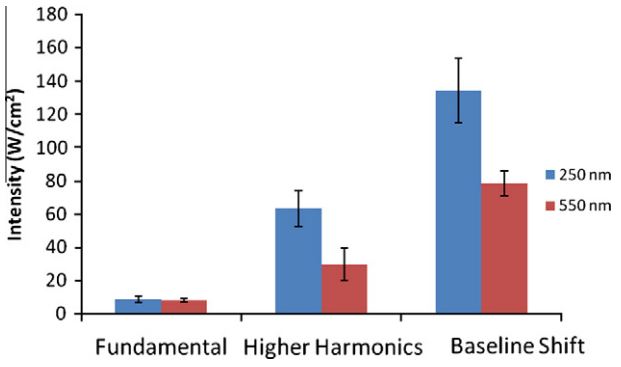

Fig. 7. Emulsion size effect on the intensity required for higher harmonics, and a baseline shift when perfluoropentane emulsions were exposed to 476 kHz US at 37 °C.

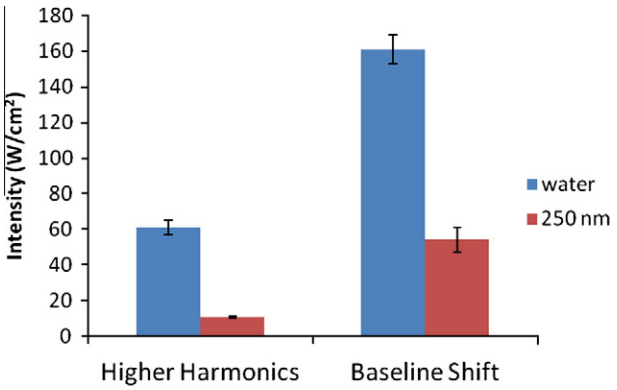

Fig. 8. Transition threshold for ddd-H_2O and 250-nm PFC_6 nanoemulsions at 476-kHz and 37 °C.

3.6. Comparison between water and nanoemulsions

The intensities for transitions in water and nanoemulsions were compared to determine if the acoustic emissions were coming from cavitation in the water surrounding the sample (and not the sample itself). If so, then the PFC emulsion and a control sample of water would have the same transition intensities. We exposed ddd-H_2O at 37 °C to 476-kHz US and recorded the intensities, when higher harmonics and a baseline shift occur. Then 250-nm perfluorohexane nanoemulsions were exposed to 476-kHz US at 37 °C. It was found that the intensity required for the appearance at higher harmonics (bubble formation) is sixfold greater than the intensity required in perfluorohexane nanoemulsions. In addition, the intensity required for inertial cavitation in water (baseline shift) is threefold the intensity required by perfluorohexane nanoemulsions (Fig. 8). The differences are significant for the onset of higher harmonics ($p < 0.0001$) and for a baseline shift ($p < 0.0001$). Similar differences were observed at 25 °C. Thus the acoustic signatures in the PFC emulsions are attributed to vaporization of the PFC phase.

3.7. Effect of frequency

We could not quantitatively study the effect of frequency because the two transducers were of different geometry. An analysis of data showed that minimum intensity required for inertial cavitation at 20 kHz is on the order of 0.4 mW/cm^2 for 550-nm PFC_6 emulsions, whereas minimum intensity required at 476 kHz is on the order of 9.84 W/cm^2 at 25 °C and 550 nm-PFC_6 emulsions. From the experimental results, we can conclude qualitatively that lower frequencies require less intensity to produce gas phase formation.

4. Conclusion

Based on our experimental results, we conclude that there is bubble formation as evidenced by higher harmonics and baseline shift in the acoustic spectrum. We studied the effect of temperature, emulsion size, and PFC species. Temperature has little effect on bubble transitions.

As for the effect of size, analysis of experimental results for PFC_6 nanoemulsions at 476 and 20 kHz revealed that larger nanoemulsions require less acoustic intensity to produce inertial cavitation.

We also attempted to deduce the effect of using the two perfluorocarbon species in generating cavitation events. The experimental results showed that PFC_6 nanoemulsions at 476 kHz required higher intensity for transitions compared to PFC_5. However, the 20-kHz experiment results showed higher intensity for PFC_5 than PFC_6.

References

[1] G.A. Husseini, W.G. Pitt, Ultrasonic-activated micellar drug delivery for cancer treatment, Journal of Pharmaceutical Sciences 98 (2009) 795–811.
[2] G.A. Husseini, W.G. Pitt, Micelles and nanoparticles for ultrasonic drug and gene delivery, Advanced Drug Delivery Reviews 60 (2008) 1137–1152.
[3] G.A. Husseini, W.G. Pitt, The use of ultrasound and micelles in cancer treatment, Journal of Nanoscience and Nanotechnology 8 (2008) 2205–2215.
[4] W.G. Pitt, Defining the role of ultrasound in drug delivery, American Journal of Drug Delivery 1 (2003) 27–42.
[5] Z. Fan, R.E. Kumon, J. Park, C.X. Deng, Intracellular delivery and calcium transients generated in sonoporation facilitated by microbubbles, Journal of Controlled Release 142 (2010) 31–39.
[6] S. Xenariou, H.D. Liang, U. Griesenbach, J. Zhu, R. Farley, L. Somerton, C. Singh, P.K. Jeffery, R.K. Scheule, S.H. Cheng, D.M. Geddes, M. Blomley, E. Alton, Low-frequency ultrasound increases non-viral gene transfer to the mouse lung, Acta Biochimica Et Biophysica Sinica 42 (2010) 45–51.
[7] G.A. Husseini, K.L. O'Neill, W.G. Pitt, The comet assay to determine the mode of cell death for the ultrasonic delivery of doxorubicin to human leukemia (HL-60 cells) from pluronic P105 micelles, Technology in Cancer Research and Treatment 4 (2005) 707–711.
[8] G.A. Husseini, C.M. Runyan, W.G. Pitt, Investigating the mechanism of acoustically activated uptake of drugs from Pluronic micelles, BMC Cancer 2 (2002).
[9] R. Suzuki, E. Namai, Y. Oda, N. Nishiie, S. Otake, R. Koshima, K. Hirata, Y. Taira, N. Utoguchi, Y. Negishi, S. Nakagawa, K. Maruyama, Cancer gene therapy by IL-12 gene delivery using liposomal bubbles and tumoral ultrasound exposure, Journal of Controlled Release 142 (2010) 245–250.
[10] C.M. Zhang, X.J. Zhang, C.B. Liu, J.F. Wang, X.H. Liu, H.L. Li, J.H. Wang, C.J. Wu, Expression of endostatin mediated by a novel non-viral delivery system inhibits human umbilical vein endothelial cells in vitro, Molecular Biology Reports 37 (2010) 1755–1762.
[11] D.J. Wells, Electroporation and ultrasound enhanced non-viral gene delivery *in vitro* and *in vivo*, Cell Biology and Toxicology 26 (2010) 21–28.
[12] E.S. Richardson, W.G. Pitt, D.J. Woodbury, The role of cavitation in liposome formation, Biophysical Journal 93 (2007) 4100–4107.
[13] G.A. Husseini, M.A.D. de la Rosa, T. Gabuji, Y. Zeng, D.A. Christensen, W.G. Pitt, Release of doxorubicin from unstabilized and stabilized micelles under the action of ultrasound, Journal of Nanoscience and Nanotechnology 7 (2007) 1028–1033.
[14] T.G. Leighton, What is ultrasound?, Progress in Biophysics & Molecular Biology 93 (2007) 3–83
[15] C.C. Church, Frequency pulse length and the mechanical index, Acoustics Research Letters Online 6 (2005) 162–168.
[16] G.A. Husseini, M.A. Diaz, E.S. Richardson, D.A. Christensen, W.G. Pitt, The role of cavitation in acoustically activated drug delivery, Journal of Controlled Release 107 (2005) 253–261.
[17] K. Yasui, J. Lee, T. Tuziuti, A. Towata, T. Kozuka, Y. Lida, Influence of the bubble–bubble interaction on destruction of encapsulated microbubbles under ultrasound, Journal of the Acoustical Society of America 126 (2009) 973–982.
[18] D. Simberg, R. Mattrey, Targeting of perfluorocarbon microbubbles to selective populations of circulating blood cells, Journal of Drug Targeting 17 (2009) 392–398.
[19] S.L. Huang, Liposomes in ultrasonic drug and gene delivery, Advanced Drug Delivery Reviews 60 (2008) 1167–1176.
[20] S. Hernot, A.L. Klibanov, Microbubbles in ultrasound-triggered drug and gene delivery, Advanced Drug Delivery Reviews 60 (2008) 1153–1166.
[21] D.L. Miller, S.V. Pislaru, J.E. Greenleaf, Sonoporation: mechanical DNA delivery by ultrasonic cavitation, Somatic Cell and Molecular Genetics 27 (2002) 115–134.
[22] D.L. Miller, O.D. Kripfgans, J.B. Fowlkes, P.L. Carson, Cavitation nucleation agents for nonthermal ultrasound therapy, Journal of the Acoustical Society of America 107 (2000) 3480–3486.
[23] D.L. Miller, WFUMB safety symposium on ehco-contrast agents: *in vitro* bioeffects, Ultrasound in Medicine and Biology 33 (2007) 197–204.
[24] M.L. Fabiilli, K.J. Haworth, I.E. Sebastian, O.D. Kripfgans, P.L. Carson, J.B. Fowlkes, Delivery of chlorambucil using an acoustically-triggered perfluoropentane emulsion, Ultrasound in Medicine and Biology 36 (2010) 1364–1375.
[25] N. Rapoport, D.A. Christensen, A.M. Kennedy, K.H. Nam, Cavitation properties of block copolymer stabilized phase-shift nanoemulsions used as drug carriers, Ultrasound in Medicine and Biology 36 (2010) 419–429.
[26] J.Y. Fang, C.F. Hung, M.H. Liao, C.C. Chien, A study of the formulation design of acoustically active lipospheres as carriers for drug delivery, European Journal of Pharmaceutics and Biopharmaceutics 67 (2010) 67–75.
[27] S.D. Caruthers, T. Cyrus, P.M. Winter, S.A. Wickline, G.M. Lanza, Anti-angiogenic perfluorocarbon nanoparticles for diagnosis and treatment of atherosclerosis, Wiley Interdisciplinary Reviews-Nanomedicine and Nanobiotechnology 1 (2009) 311–323.
[28] S.L. Huang, D.B. McPherson, R.C. MacDonald, A method to co-encapsulate gas and drugs in liposomes for ultrasound-controlled drug delivery, Ultrasound in Medicine and Biology 34 (2008) 1272–1280.
[29] N.R. Soman, J.N. Marsh, G.M. Lanza, S.A. Wickline, New mechanisms for non-porative ultrasound stimulation of cargo delivery to cell cytosol with targeted perfluorocarbon nanoparticles, Nanotechnology 19 (2008).
[30] H.S. Choi, J.F. Ma, Use of perfluorocarbon compound in the endorectal coil to improve MR spectroscopy of the prostate, American Journal of Roentgenology 190 (2008) 1055–1059.
[31] J. Holzfuss, Acoustic energy radiated by nonlinear spherical oscillations of strongly driven bubbles, Proceedings of the Royal Society A-Mathematical Physical and Engineering Sciences 466 (2010) 1829–1847.
[32] J.H. Bang, K.S. Suslick, Applications of ultrasound to the synthesis of nanostructured materials, Advanced Materials 22 (2010) 1039–1059.
[33] A.R. Klotz, L. Lindvere, B. Stefanovic, K. Hynynen, Temperature change near microbubbles within a capillary network during focused ultrasound, Physics in Medicine and Biology 55 (2010) 1549–1561.
[34] T.M. Krupka, L. Solorio, R.E. Wilson, H.P. Wu, N. Azar, A.A. Exner, Formulation and characterization of echogenic lipid-pluronic nanobubbles, Molecular Pharmaceutics 7 (2010) 49–59.
[35] M. Nishihara, K. Imai, M. Yokoyama, Preparation of perfluorocarbon/fluoroalkyl polymer nanodroplets for cancer-targeted ultrasound contrast agents, Chemistry Letters 38 (2009) 556–557.
[36] L.W. Seymour, Passive tumor targeting of soluble macromolecules and drug conjugates, Critical Reviews in Therapeutic Drug Carrier Systems 9 (1992) 135–187.
[37] G.A. Husseini, M.A.D. de la Rosa, E.S. Richardson, D.A. Christensen, W.G. Pitt, The role of cavitation in acoustically activated drug delivery, Journal of Controlled Release 107 (2005) 253–261.
[38] T.G. Leighton, The Acoustic Bubble, Academic Press, London, 1994.
[39] G.A. Husseini, M.A. Diaz de la Rosa, T. Gabuji, Y. Zeng, D.A. Christensen, W.G. Pitt, Release of doxorubicin from unstabilized and stabilized micelles under the action of ultrasound, Journal of Nanoscience and Nanotechnology 7 (2007) 1–6.